ELSEVIER

Influence of the direction of motion on the inelastic interaction between electrons and solid surfaces

Y.C. Li [a], Y.H. Tu [a], C.M. Kwei [a,*], C.J. Tung [b]

[a] *Department of Electronics Engineering, National Chiao Tung University, Hsinchu 300, Taiwan*
[b] *Department of Nuclear Science, National Tsing Hua University, Hsinchu 300, Taiwan*

Abstract

Theoretical derivations of the inelastic differential inverse mean free path (DIMFP) and inelastic mean free path (IMFP) for electrons crossing solid surfaces were made for different crossing angles and electron distances relative to the crossing point at the surface. Individual contributions from volume and surface excitations were separated and analyzed for electrons traveling inside and outside the solid. Extended Drude dielectric functions were employed to calculate the DIMFP and inverse IMFP for electrons incident into and escaping from Cu. It was found that the DIMFP and inverse IMFP for electrons moving inside the solid were approximately independent of crossing angle and position of electrons due to the compensation of volume and surface excitations. For electrons moving deep inside the solid, the DIMFP and inverse IMFP reduced to the values for electrons moving in an infinite solid. As electrons traveling in the vacuum, the DIMFP and inverse IMFP became greater for glancing incident and escaping angles since surface excitations were more probable. The surface excitation parameter (SEP) for electrons traveling in vacuum showed an angular dependence. The SEP of escaping electrons was found larger than that of incident electrons due to the attractive force exerted by the induced surface charges. The calculated SEP was found to follow a simple expression.
© 2005 Elsevier B.V. All rights reserved.

Keywords: Electron; Inelastic mean free path; Surface excitation; Volume excitation

1. Introduction

Quantitative information on inelastic interaction cross-sections of low-energy electrons crossing solid surfaces is important in surface sensitive spectroscopies such as Auger electron spectroscopy

* Corresponding author. Tel.: +886 3 5712121x54136; fax: +886 3 5727300.
 E-mail address: cmkwei@cc.nctu.edu.tw (C.M. Kwei).

(AES), X-ray photoelectron spectroscopy (XPS) and reflection electron energy-loss spectroscopy (REELS), etc. This information can be extracted from experimentally measured REELS spectra by the deconvolution method [1]. The extracted inelastic cross-sections contain the combined effects arisen from volume and surface plasmon excitations. Volume excitations occur for electrons traveling inside the solid. Surface excitations originate from electrons, either inside or outside the solid, moving at a distance in the order of angstroms from the surface. Within the solid, the decrease in volume excitations as electrons move close to the surface is compensated by the increase in surface excitations. This makes the total inelastic cross-section at any position inside the solid nearly independent of depth [2,3]. For electrons traveling outside the solid, only surface excitations are attainable over an effective region close to the surface [3]. In such a case, the surface excitations are usually characterized by the so-called surface excitation parameter (SEP), defined as the average number of surface plasmons excited by electrons outside the solid [3]. Tougaard and Chorkendorff [1] extracted the inelastic cross-sections from the REELS spectra without separating out the contribution of surface excitations. Chen [4] singled out this contribution by incorporating a surface effect into the Landau formula in the deconvolution method and applying an approximate relation of $\frac{1}{\sqrt{E}}$ for the energy dependence to the surface excitation probability.

Theoretical derivations of inelastic cross-sections for low-energy electrons crossing solid surfaces have been made using the dielectric response theory [2,3,5]. Yubero et al. [6–8] derived the effective (or lumped) inelastic cross-sections for backscattered electrons assuming a single-elastic backward-scattering in the trajectory of the electron. In reality, the electron might experience plural or multiple elastic scatterings in its trajectory before being scattered out of the solid. In spite of this, the effective inelastic cross-sections of Yubero et al. were compared well with experimentally determined inelastic cross-sections. The effective inelastic cross-sections contain information on reflected electrons that cross the surface twice. Because it is difficult to separate out the contribution

of surface excitations from the lumped cross-sections, the effective cross-sections should not be applied directly to the quantitative analysis of XPS and AES for which electrons cross the surface only once. Simonsen et al. [9] later proposed a model which included the effect of static core hole for XPS and AES. In this model, the trajectory of the electron was assumed to follow a straight line due to its neglect of elastic scatterings. Elastic scatterings, however, are important in the REELS analyses. In the present work, attempts were made to develop position-dependent inelastic cross-sections for obliquely incident and escaping electrons that were applicable to the REELS analyses.

Recently, the present authors developed a dielectric response function model [10] to calculate the depth-dependent differential inverse mean free path (DIMFP), the inelastic mean free path (IMFP) and surface excitation parameter (SEP) for electrons normally crossing through solid surfaces [3]. For other crossing angle α, the SEP values were found by multiplying the results on SEP for normally crossing angle with $(\cos\alpha)^{-1}$ [3,11]. However, momentum transfer in cylindrical coordinates with no restriction on its normal component was adopted for performing the momentum integration in the model. The conservations of energy and momentum were not completely satisfied, and the derived DIMFP for volume excitations in the limit of large depths did not match the DIMFP in an infinite solid.

In the present work, a similar approach as that in the previous model [2,3] was followed to determine the angular dependence of inelastic cross-sections for electrons incident into or escaping from the solid. Spherical coordinates were employed in the momentum integration to satisfy the energy and momentum conservations [12]. Further, the dependences of DIMFP and inverse IMFP on the crossing angle and the position of electrons were established from first principles based on the extended Drude dielectric functions [10]. The angular distribution of SEP was also investigated. Calculated SEPs for copper were fitted to an analytical formula. A comparison was made between presently calculated results and corresponding data of other models [11,13,14].

2. Methods

As illustrated in Fig. 1, an electron of charge e and velocity $\vec{v}$ travels across an interface at time $t = 0$ from medium 1 of dielectric function $\varepsilon_1(\vec{q}, \omega)$ to medium 2 of dielectric function $\varepsilon_2(\vec{q}, \omega)$, where $\vec{q}$ is the momentum transfer and ω is the energy transfer. Note that atomic units are used throughout this paper unless otherwise specified. The crossing angle α is defined as the angle between the interface normal and the electron moving direction. The instant position of the electron is $\vec{r} = \vec{v}t$, relative to the crossing point at the interface. As the electron crosses the interface, surface and volume excitations are probable due to electron–solid interactions. Surface excitations occur when the electron travels near the interface, while volume excitations arise as the electron moves inside the media. These two excitations can be described using the dielectric response theory [2,3]. By solving the Poisson's equation, the Fourier components of the scalar potentials in media 1 and 2 are given by [3,15]

$$\Phi^{(1)}(\vec{q}, \omega) = \frac{-8\pi^2}{q^2 \varepsilon_1(\vec{q}, \omega)} \left[\delta(\omega - qv\cos\beta) + \rho_s(\vec{Q}, \omega) \right]$$
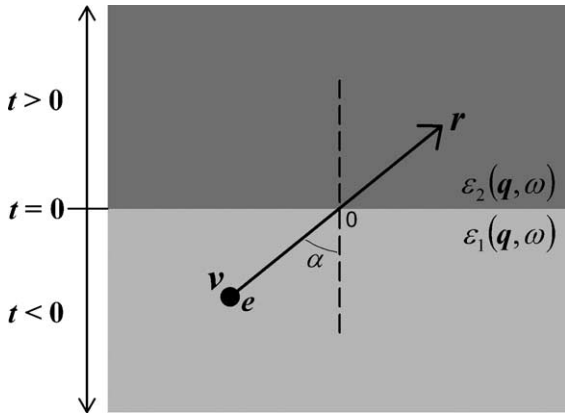$$\text{for } t < 0 \tag{1}$$

Fig. 1. A sketch of the problem studied in this work. An electron of velocity $\vec{v}$ moves across the interface at time $t = 0$ from medium 1 of dielectric function $\varepsilon_1(\vec{q}, \omega)$ to medium 2 of dielectric function $\varepsilon_2(\vec{q}, \omega)$ with crossing angle α. The instant position of the electron is $\vec{r} = \vec{v}t$, relative to the crossing point at interface.

and

$$\Phi^{(2)}(\vec{q}, \omega) = \frac{-8\pi^2}{q^2 \varepsilon_2(\vec{q}, \omega)} \left[\delta(\omega - qv\cos\beta) - \rho_s(\vec{Q}, \omega) \right]$$
$$\text{for } t > 0, \tag{2}$$

where $\vec{q} = (\vec{Q}, q_z)$, $\vec{Q}$ and q_z are the parallel and normal components of $\vec{q}$ with respect to the surface, β is the angle between $\vec{q}$ and $\vec{v}$, and $\rho_s(\vec{Q}, \omega)$ is the induced surface charge density. The signs accompanying the induced surface charge density are opposite for $t < 0$ and for $t > 0$, which is due to the requirement for the continuity of the normal component of the electric displacement at the interface. The other boundary condition, i.e. the continuity of the tangential components of the electric field at the interface, requires that the induced surface charge density follows:

$$\rho_s(\vec{Q}, \omega) = \frac{\int_{-\infty}^{+\infty} \frac{\delta(\omega - \vec{Q}\cdot\vec{v}_\parallel - q_z v_\perp)}{q^2} \left[\frac{1}{\varepsilon_2(\vec{q}, \omega)} - \frac{1}{\varepsilon_1(\vec{q}, \omega)} \right] \mathrm{d}q_z}{\int_{-\infty}^{+\infty} \frac{1}{q^2} \left[\frac{1}{\varepsilon_2(\vec{q}, \omega)} + \frac{1}{\varepsilon_1(\vec{q}, \omega)} \right] \mathrm{d}q_z},$$
$$\tag{3}$$

where $v_\perp$ and $v_\parallel$ are the normal and parallel components of $\vec{v}$ with respect to the surface.

Now the Fourier components of the scalar potentials, $\Phi^{(1)}(\vec{q}, \omega)$ and $\Phi^{(2)}(\vec{q}, \omega)$ on either side of the interface, can be obtained after substituting Eq. (3) into Eqs. (1) and (2). The induced potentials in real space can be derived by the inverse Fourier transforms of $\Phi^{(1)}(\vec{q}, \omega)$ and $\Phi^{(2)}(\vec{q}, \omega)$ after removing the potential of the electron in vacuum. Adopting spherical coordinates in the integration of momentum transfer, the induced potentials can be written as

$$\Phi_{\text{ind}}^{(1)}(\vec{r}, t) = -\frac{1}{\pi} \int \int \int \delta(\omega - qv\cos\beta) \left[\frac{1}{\varepsilon_1(\vec{q}, \omega)} - 1 \right]$$
$$\times \mathrm{e}^{\mathrm{i}(qvt\cos\beta - \omega t)} \sin\beta \, \mathrm{d}\beta \, \mathrm{d}q \, \mathrm{d}\omega$$
$$- \frac{1}{2\pi^2} \int \int \int \int \frac{\rho_s(\vec{Q}, \omega)}{\varepsilon_1(\vec{q}, \omega)} \mathrm{e}^{\mathrm{i}(\vec{Q}\cdot\vec{R} - \omega t)}$$
$$\times \mathrm{e}^{\mathrm{i}q_z z} \sin\theta \, \mathrm{d}\phi \, \mathrm{d}\theta \, \mathrm{d}q \, \mathrm{d}\omega \quad \text{for } t < 0 \tag{4}$$

and

$$\Phi_{\text{ind}}^{(2)}(\vec{r},t) = -\frac{1}{\pi} \int \int \int \delta(\omega - qv\cos\beta)\left[\frac{1}{\varepsilon_2(\vec{q},\omega)} - 1\right]$$
$$\times \, \mathrm{e}^{\mathrm{i}(qvt\cos\beta - \omega t)} \sin\beta \, \mathrm{d}\beta \, \mathrm{d}q \, \mathrm{d}\omega$$
$$+ \frac{1}{2\pi^2} \int \int \int \int \frac{\rho_s(\vec{Q},\omega)}{\varepsilon_2(\vec{q},\omega)} \mathrm{e}^{\mathrm{i}(\vec{Q}\cdot\vec{R} - \omega t)}$$
$$\times \, \mathrm{e}^{\mathrm{i}q_z z} \sin\theta \, \mathrm{d}\phi \, \mathrm{d}\theta \, \mathrm{d}q \, \mathrm{d}\omega \quad \text{for } t > 0,$$

$$(5)$$

where $\vec{r} = (\vec{R}, z)$, $\vec{R}$ and z are the parallel and normal components of $\vec{r}$ with respect to the surface, and

$$\frac{\rho_s(\vec{Q},\omega)}{\varepsilon_j(\vec{q},\omega)} = \frac{1}{\pi} \frac{Qv_\perp}{(\omega - \vec{Q}\cdot\vec{v}_\parallel)^2 + Q^2 v_\perp^2}$$
$$\times \frac{\varepsilon_1(\vec{Q},\omega) - \varepsilon_2(\vec{Q},\omega)}{\varepsilon_j(\vec{Q},\omega)\left[\varepsilon_1(\vec{Q},\omega) + \varepsilon_2(\vec{Q},\omega)\right]}$$
$$\text{for } j = 1 \text{ and } 2. \quad (6)$$

Eq. (6) was derived under the assumption that $\varepsilon(\vec{q},\omega) \approx \varepsilon(\vec{Q},\omega)$ [6,7]. The integrations over ω in the second integrals of Eqs. (4) and (5) can be performed by closing the contour in the upper and lower half planes for $t < 0$ and $t > 0$, respectively. To carry out the contour integration in the lower half plane, it is convenient to convert it into the upper half plane by replacing $\mathrm{e}^{\mathrm{i}(\vec{Q}\cdot\vec{R} - \omega t)}$ in Eq. (5) with $\mathrm{e}^{\mathrm{i}(\vec{Q}\cdot\vec{R} - \omega t)} = 2\cos(\omega t - \vec{Q}\cdot\vec{R}) - \mathrm{e}^{-\mathrm{i}(\vec{Q}\cdot\vec{R} - \omega t)}$. The stopping power, $-\frac{\mathrm{d}W}{\mathrm{d}s}$, can be related to the induced potential, $\Phi_{\text{ind}}(\vec{r},t)$, by [16]

$$-\frac{\mathrm{d}W}{\mathrm{d}s} = \frac{1}{v}\left[\frac{\partial \Phi_{\text{ind}}(\vec{r},t)}{\partial t}\right]_{\vec{r}=\vec{v}t}, \quad (7)$$

where the derivative of the induced potential is evaluated at the position of the electron. And the stopping power can be expressed in terms of the position-dependent DIMFP, $\mu(\alpha, E, \omega, r)$, according to

$$-\frac{\mathrm{d}W}{\mathrm{d}s} = \int_0^E \omega \mu(\alpha, E, \omega, r) \, \mathrm{d}\omega. \quad (8)$$

In the case of an electron traveling from solid to vacuum, i.e. $s \to v$, $\varepsilon_1(\vec{q},\omega)$ and $\varepsilon_2(\vec{q},\omega)$ may be replaced by $\varepsilon(\vec{q},\omega)$ and 1, respectively. The DIMFP is therefore given by

$$\mu^{\text{s}\to\text{v}}(\alpha, E, \omega, r)$$
$$= \frac{2}{\pi v^2} \int_{q_-}^{q_+} \mathrm{d}q \frac{1}{q} \mathrm{Im}\left[\frac{-1}{\varepsilon(\vec{q},\omega)}\right]\Theta(-r)$$
$$- \frac{2\cos\alpha}{\pi^3} \int_{q_-}^{q_+} \mathrm{d}q \int_0^{\pi/2} \mathrm{d}\theta \int_0^{2\pi} \mathrm{d}\phi$$
$$\times \frac{q\sin^2\theta \cos(q_z r \cos\alpha) \exp(-|r|Q\cos\alpha)}{\tilde{\omega}^2 + Q^2 v_\perp^2}$$
$$\times \mathrm{Im}\left[\frac{-1}{\varepsilon(\vec{Q},\omega)}\right]\Theta(-r) + \frac{4\cos\alpha}{\pi^3}\int_{q_-}^{q_+}\mathrm{d}q$$
$$\times \int_0^{\pi/2}\mathrm{d}\theta \int_0^{2\pi}\mathrm{d}\phi$$
$$\times \frac{q\sin^2\theta \cos(q_z r \cos\alpha)\exp(-|r|Q\cos\alpha)}{\tilde{\omega}^2 + Q^2 v_\perp^2}$$
$$\times \mathrm{Im}\left[\frac{-1}{\varepsilon(\vec{Q},\omega)+1}\right]\Theta(-r)$$
$$+ \frac{4\cos\alpha}{\pi^3}\int_{q_-}^{q_+}\mathrm{d}q\int_0^{\pi/2}\mathrm{d}\theta\int_0^{2\pi}\mathrm{d}\phi$$
$$\times \frac{q\sin^2\theta \exp(-|r|Q\cos\alpha)}{\tilde{\omega}^2 + Q^2 v_\perp^2}\mathrm{Im}\left[\frac{-1}{\varepsilon(\vec{Q},\omega)+1}\right]$$
$$\times \left[2\cos\left(\frac{\tilde{\omega}r}{v}\right) - \exp(-|r|Q\cos\alpha)\right]\Theta(r),$$

$$(9)$$

where $\tilde{\omega} = \omega - qv\sin\theta\cos\phi\sin\alpha$, $Q = q\sin\theta$, $q_z = q\cos\theta$, $v_\perp = v\cos\alpha$, $E = \frac{v^2}{2}$, and $\Theta(r)$ is the Heaviside step function. Applying the energy–momentum conservation relations, the upper and lower limits of q are $q_\pm = \sqrt{2E} \pm \sqrt{2(E - \omega)}$. The terms involving $\mathrm{Im}(\frac{-1}{\varepsilon+1})$ are due to the contribution from surface excitations, whereas those involving $\mathrm{Im}(\frac{-1}{\varepsilon})$ are contributed from volume excitations. Eq. (9) reveals that only surface excitations are possible for the electron traveling outside the solid. However, both volume and surface excitations may occur for the electron moving inside the solid. The term $\exp(-|r|Q\cos\alpha)$ in Eq. (9) indicates that the contribution from surface excitations decreases exponentially with the increase in distance from the surface. On the other hand, the reduction in the contribution from volume excitations increases rapidly as the electron moves near the surface. When electron moves deep inside the solid, i.e.

$r \to -\infty$, Eq. (9) reduces to the same expression as that for an electron moving in the infinite solid. The inverse IMFP for an escaping electron can be calculated using

$$\mu^{s \to v}(\alpha, E, r) = \int_0^E \mu^{s \to v}(\alpha, E, \omega, r) d\omega. \tag{10}$$

For an electron moving outside the solid, the SEP may be obtained by integrating the inverse IMFP over the whole path length of the electron. Thus the SEP for escaping electrons is given by

$$P_s^{s \to v}(\alpha, E) = \int_0^\infty \mu^{s \to v}(\alpha, E, r) dr. \tag{11}$$

Similar derivations can be performed for an electron entering the solid by taking $\varepsilon_1(\vec{q}, \omega) = 1$ and $\varepsilon_2(\vec{q}, \omega) = \varepsilon(\vec{q}, \omega)$. In this case, i.e. v → s, the DIMFP for the incident electron is given by

$$
\begin{aligned}
\mu^{v \to s}(\alpha, E, \omega, r) =& \frac{4\cos\alpha}{\pi^3} \int_{q_-}^{q_+} dq \int_0^{\pi/2} d\theta \\
&\times \int_0^{2\pi} d\phi \frac{q\sin^2\theta\cos(q_z r\cos\alpha)}{\tilde{\omega}^2 + Q^2 v_\perp^2} \\
&\times \exp(-|r|Q\cos\alpha)\text{Im}\left[\frac{-1}{\varepsilon(\vec{Q}, \omega)+1}\right]\Theta(-r) \\
&+ \frac{2}{\pi v^2} \int_{q_-}^{q_+} dq \frac{1}{q}\text{Im}\left[\frac{-1}{\varepsilon(\vec{q}, \omega)}\right]\Theta(r) \\
&- \frac{2\cos\alpha}{\pi^3} \int_{q_-}^{q_+} dq \int_0^{\pi/2} d\theta \\
&\times \int_0^{2\pi} d\phi \frac{q\sin^2\theta\exp(-|r|Q\cos\alpha)}{\tilde{\omega}^2 + Q^2 v_\perp^2} \\
&\times \text{Im}\left[\frac{-1}{\varepsilon(\vec{Q}, \omega)}\right]\left[2\cos\left(\frac{\tilde{\omega}r}{v}\right)\right. \\
&\left. -\exp(-|r|Q\cos\alpha)\right]\Theta(r) \\
&+ \frac{4\cos\alpha}{\pi^3} \int_{q_-}^{q_+} dq \int_0^{\pi/2} d\theta \\
&\times \int_0^{2\pi} d\phi \frac{q\sin^2\theta\exp(-|r|Q\cos\alpha)}{\tilde{\omega}^2 + Q^2 v_\perp^2} \\
&\times \text{Im}\left[\frac{-1}{\varepsilon(\vec{Q}, \omega)+1}\right]\left[2\cos\left(\frac{\tilde{\omega}r}{v}\right)\right. \\
&\left. -\exp(-|r|Q\cos\alpha)\right]\Theta(r). \tag{12}
\end{aligned}
$$

Corresponding inverse IMFP and SEP can be obtained from

$$\mu^{v \to s}(\alpha, E, r) = \int_0^E \mu^{v \to s}(\alpha, E, \omega, r) d\omega \tag{13}$$

and

$$P_s^{v \to s}(\alpha, E) = \int_{-\infty}^0 \mu^{v \to s}(\alpha, E, r) dr. \tag{14}$$

Letting $\alpha = 0°$ in Eqs. (9) and (12), formulas for normally escaping and incident electrons exhibit similarities between present and previous works [2,3]. The difference between these works is attributed to the application of momentum–energy conservations. In the previous work, the integration over the normal component of the momentum transfer, q_z, was not restricted by the conservation relations. In the present work, however, these relations are completely satisfied by electron–solid inelastic interaction cross-sections using spherical coordinates.

3. Results and discussion

Using Eqs. (9)–(14) and the extended Drude dielectric functions, we have calculated the DIMFP, inverse IMFP and SEP for an electron entering or escaping from the solid. Fitting parameters of the dielectric functions were taken from our previous work [10]. Figs. 2 and 3 show the results of calculations on the DIMFP for a 500 eV electron escaping from Cu to vacuum with various electron distances from the surface crossing point, r, either outside (Fig. 2) or inside (Fig. 3) Cu for different crossing angles, α. When the electron is in the vacuum, Fig. 2 shows that the DIMFP is entirely contributed from surface excitations. As the electron moves away from the surface, corresponding to larger r values, the DIMFP becomes smaller due to the decrease in surface excitations. The DIMFP becomes larger for greater α values at a fixed r value because of the shorter distance to the surface. The characteristic surface plasmon energy, or the peak energy loss, is nearly independent of the crossing angle and the electron distance from the crossing point. For the electron inside the
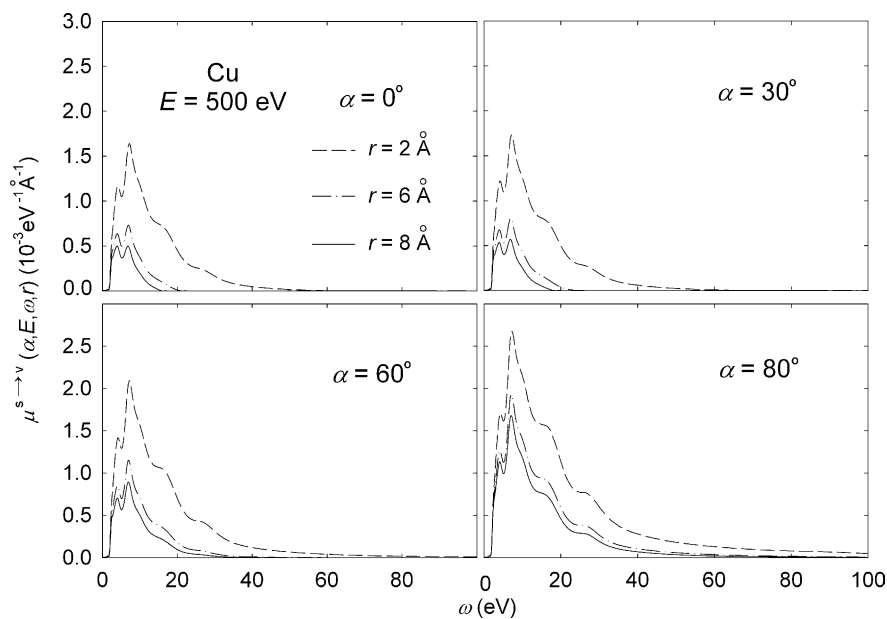
Fig. 2. Calculated results of the DIMFP in vacuum for a 500 eV escaping electron from Cu to vacuum with different crossing angles and distances from the crossing point at the surface.
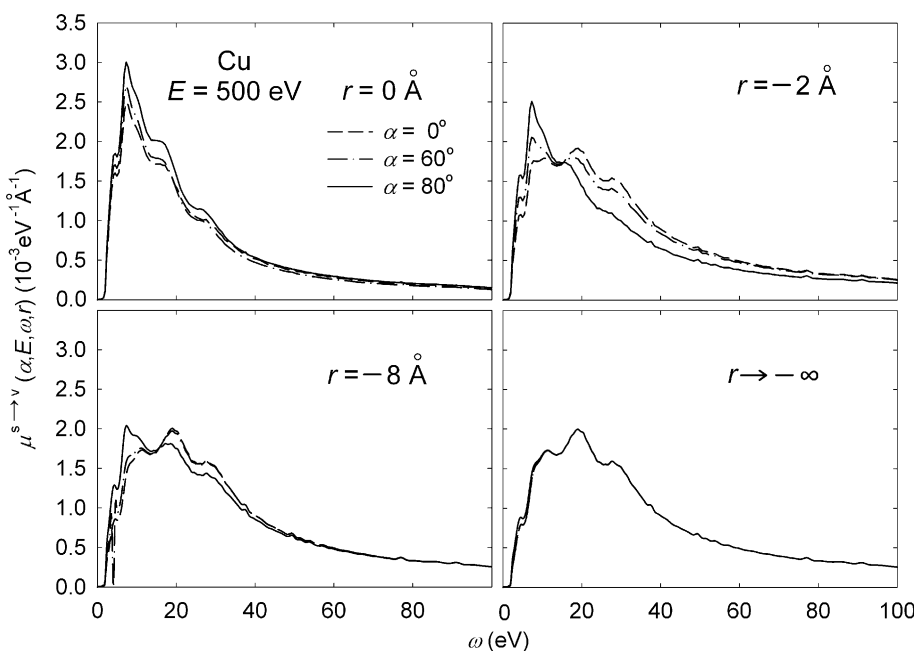

Fig. 3. Calculated results of the DIMFP in Cu for a 500 eV escaping electron from Cu to vacuum with different crossing angles and distances from the crossing point at the surface.

solid, Fig. 3 shows that the DIMFP also varies with electron distance from the crossing point. Here the DIMFP exhibits broad peaks due to the overlapping of the contributions from surface and volume excitations. Inside the solid, the DIMFP is either weakly dependent or independent of the crossing angle. This DIMFP quickly reduces to the asymptotic value for an electron moving in the infinite solid. This reveals that surface excitations are essentially possible only in a limited region near the surface. Similar results on the DIMFP for a 500 eV incident electron moving from vacuum to Cu are plotted in Figs. 4 and 5 for the electron moving outside and inside Cu, respectively. Again, surface excitations are important when the electron moves near the surface. In the case of the electron moving in vacuum, the DIMFP is enhanced for glancing incident angles. For the electron moving in solid, this angular dependence becomes relatively weak.

Using Eq. (10), we have calculated the inverse IMFP for a 500 eV electron escaping from Cu to vacuum as a function of electron distance relative to the surface crossing point. Results are plotted

in Fig. 6 for different crossing angles. As the electron travels outside the solid, i.e. $r > 0$, the inverse IMFP falls off rapidly, especially for smaller crossing angles. This indicates that the glancing escaping electron is more likely to induce surface excitations than the normally escaping electron because the former electron spends longer time near the surface. For the electron traveling inside the solid, i.e. $r < 0$, the inverse IMFP is roughly independent of electron distance and crossing angle due to the approximate compensation of volume and surface excitations. Therefore, the total inverse IMFP of the electron inside the solid can be approximated by a constant value equal to the inverse IMFP for the infinite solid. A similar plot of the inverse IMFP for a 500 eV incident electron moving from vacuum to Cu is shown in Fig. 7 for several crossing angles. Here the inverse IMFP of the incident electron in vacuum, i.e. $r < 0$, is smaller than that of the escaping electron in vacuum shown in Fig. 6. This is because the attractive force acting on the incident electron in vacuum by the induced surface charges is parallel to electron moving direction and thus accelerates
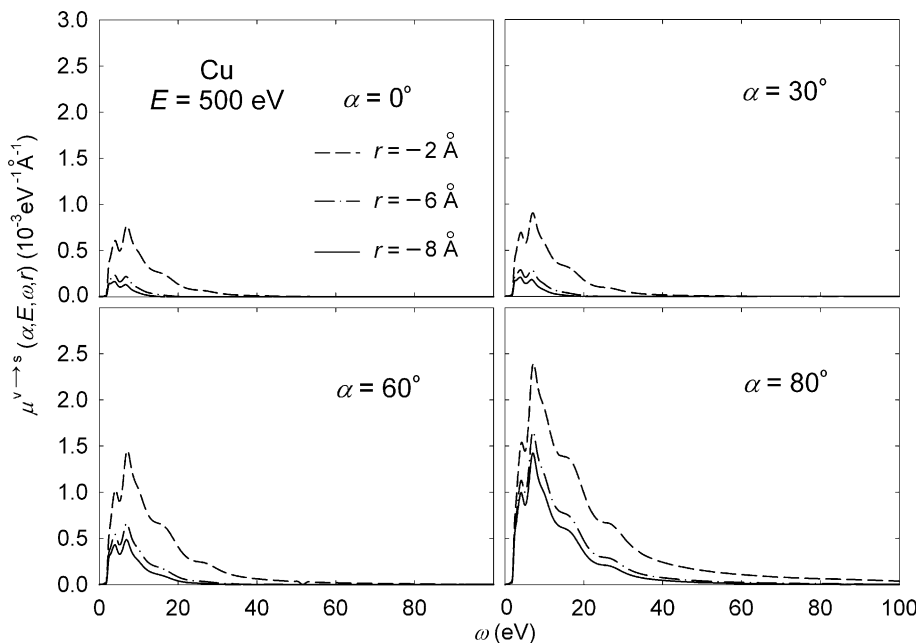

Fig. 4. Calculated results of the DIMFP in vacuum for a 500 eV incident electron from vacuum to Cu with different crossing angles and distances from the crossing point at the surface.
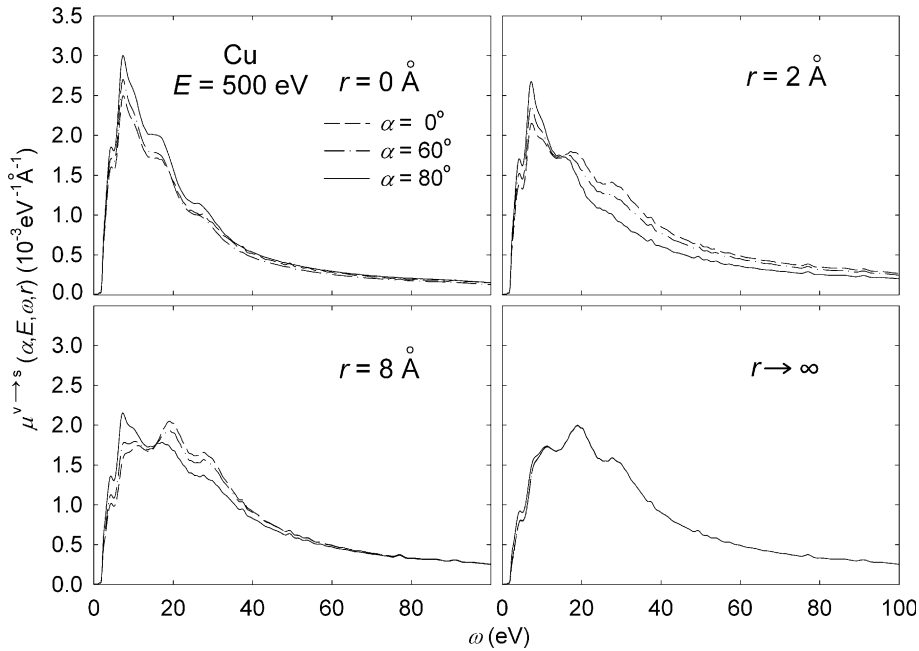
Fig. 5. Calculated results of the DIMFP in Cu for a 500 eV incident electron from vacuum to Cu with different crossing angles and distances from the crossing point at the surface.
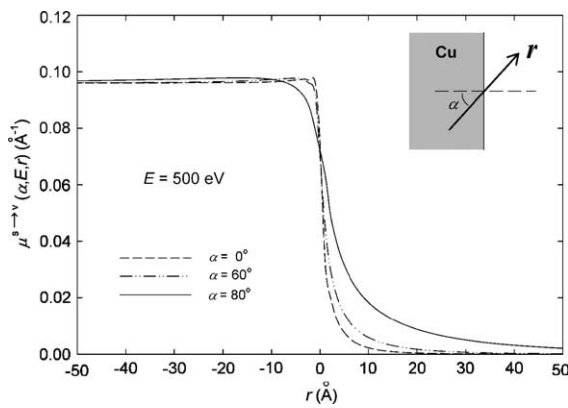

Fig. 6. A plot of the inverse IMFP for a 500 eV escaping electron from Cu to vacuum with different crossing angles as a function of electron distance from the crossing point at the surface.
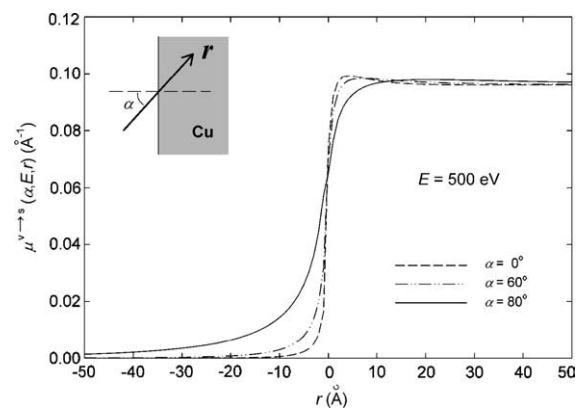
Fig. 7. A plot of the inverse IMFP for a 500 eV incident electron from vacuum to Cu with different crossing angles as a function of electron distance from the crossing point at the surface.

the electron. On the other hand, the attractive force on the escaping electron in vacuum is antiparallel to electron moving direction and hence decelerates the electron. Therefore, the time spent near the surface for incident electron is less than

that for escaping electron, leading to less surface excitations for incident electron.

Fig. 8 shows the results (solid circles) of the angular dependent SEP calculated using Eq. (11) for a 500 eV electron escaping from Cu to vacuum.
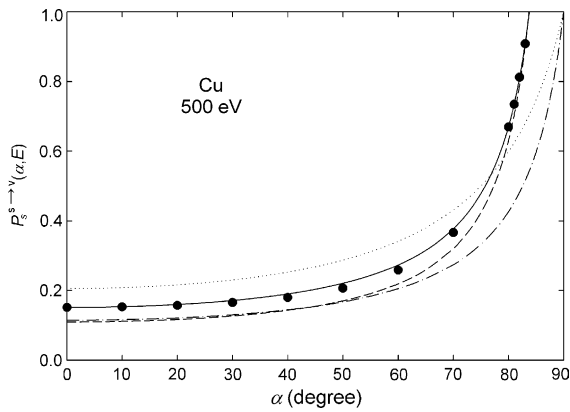
Fig. 8. A plot of the SEP for a 500 eV escaping electron from Cu to vacuum as a function of crossing angle. Symbols are the calculated results using Eq. (11). Solid curve is the fitting results using Eq. (15). Corresponding data of Chen (dashed curve), Oswald (dotted curve) and Werner et al. (dash-dot curve) are plotted for comparisons.
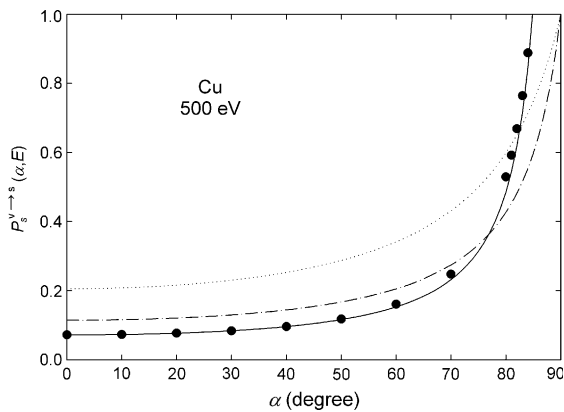

Fig. 9. A plot of the SEP for a 500 eV incident electron from vacuum to Cu as a function of crossing angle. Symbols are the calculated results using Eq. (14). Solid curve is the fitting results using Eq. (15). Corresponding data of Oswald (dotted curve) and Werner et al. (dash-dot curve) are plotted for comparisons.

Similar results (solid circles) calculated using Eq. (14) are plotted in Fig. 9 for a corresponding incident electron from vacuum to Cu. It can be seen that the SEP rises slowly with increasing crossing angle until about $\alpha = 70°$, above which such a rise becomes rapidly. Examining the calculated results, the SEP is found to follow an equation:

$$P_{\mathrm{s}}^{\mathrm{s}\to\mathrm{v}}(\alpha, E) \quad \text{or} \quad P_{\mathrm{s}}^{\mathrm{v}\to\mathrm{s}}(\alpha, E) = \frac{a(E)}{\cos^b \alpha}. \tag{15}$$

The best-fitted values of the parameters are $a = 0.1516$ and $b = 0.85$ for 500 eV escaping electrons and $a = 0.0720$ and $b = 1.09$ for 500 eV incident electrons. The fitting results are also plotted in Figs. 8 and 9 as solid curves. A comparison between Figs. 8 and 9 indicates that the SEP is larger for escaping electrons than for incident electrons, an effect mentioned above. Also, results of Oswald [13] (dotted curve), Werner et al. [14,17,18] (dash-dot curve) and Chen [11] (dashed curve) are included in these figures for comparisons. Some discrepancies among all theoretical results are found. In spite of the differences in magnitude for the SEP, the angular dependences are all similar for α less than 60°. For α more than 60°, the angular dependences are also similar for the present results of escaping electrons and the results of Werner et al. The fitted formula by Chen [11] is available only for escaping electrons. Our present fittings are made for both incident and escaping electrons. Here we find that the angular dependence of the SEP does not follow the $(\cos\alpha)^{-1}$ law but follows Eq. (15).

4. Conclusions

Based on the dielectric response theory, a theoretical derivation was made to calculate the position-dependent inelastic cross-sections for electrons moving across a solid surface at different crossing angles. Formulas were derived for both incident and escaping electrons using spherical coordinates that completely satisfied the conservation constraints of energy and momentum. Calculations of these cross-sections were performed using the extended Drude dielectric functions derived from optical data. It was found that the DIMFP and inverse IMFP for electrons moving inside the solid were approximately independent of the crossing angle and position of electrons owing to the approximate compensation of volume and surface excitations. For electrons moving deep inside the solid, the calculated DIMFP and inverse IMFP reduced to the values for electrons moving in an infinite solid. As electrons traveling in the vacuum, the DIMFP and inverse IMFP became larger for glancing incident and escaping angles

since surface excitations were more probable than for normally incident and escaping angles. The SEP of escaping electrons was found larger than that of incident electrons due to the attractive force exerted by the induced surface charges. The presently calculated SEP was found to follow a simple expression valid for practical applications. The consideration of SEP in the intensity reduction for reflected and emitted electrons is important in experimental and theoretical surface and interface analyses.

Acknowledgement

References

[1] S. Tougaard, I. Chorkendorff, Phys. Rev. B 35 (1987) 6570.
[2] Y.F. Chen, C.M. Kwei, Surf. Sci. 364 (1996) 131.
[3] C.M. Kwei, C.Y. Wang, C.J. Tung, Surf. Interface Anal. 26 (1998) 682.
[4] Y.F. Chen, Phys. Rev. B 58 (1998) 8087.
[5] C.J. Tung, Y.F. Chen, C.M. Kwei, T.L. Chou, Phys. Rev. B 49 (1994) 16684.
[6] F. Yubero, S. Tougaard, Phys. Rev. B 46 (1992) 2486.
[7] F. Yubero, J.M. Sanz, B. Ramskov, S. Tougaard, Phys. Rev. B 53 (1996) 9719.
[8] F. Yubero, D. Fujita, B. Ramskov, S. Tougaard, Phys. Rev. B 53 (1996) 9728.
[9] A.C. Simonsen, F. Yubero, S. Tougaard, Phys. Rev. B 56 (1997) 1612.
[10] C.M. Kwei, Y.F. Chen, C.J. Tung, J.P. Wang, Surf. Sci. 293 (1993) 202.
[11] Y.F. Chen, Surf. Sci. 519 (2002) 115.
[12] C.M. Kwei, S.J. Hwang, Y.C. Li, C.J. Tung, J. Appl. Phys. 93 (2003) 9130.
[13] R. Oswald, Ph.D. Thesis, University of Tübingen, Tübingen, 1997.
[14] W.S.M. Werner, W. Smekal, C. Tomastik, H. Störi, Surf. Sci. 486 (2001) L461.
[15] C.M. Kwei, S.Y. Chiou, Y.C. Li, J. Appl. Phys. 85 (1999) 8247.
[16] F. Flores, F. Garcia-Moliner, J. Phys. C 12 (1979) 907.
[17] W.S.M. Werner, W. Smekal, H. Störi, Surf. Interface Anal. 31 (2001) 475.
[18] W.S.M. Werner, C. Eisenmenger-Sittner, J. Zemek, P. Jiricek, Phys. Rev. B 67 (2003) 155412.